

Robust Total Least Mean M-Estimate normalized subband filter Adaptive Algorithm for impulse noises and noisy inputs

Haiquan Zhao, *Senior Member, IEEE*, Zian Cao, and Yida Chen

Abstract—When the input signal is correlated input signals, and the input and output signal is contaminated by Gaussian noise, the total least squares normalized subband adaptive filter (TLS-NSAF) algorithm shows good performance. However, when it is disturbed by impulse noise, the TLS-NSAF algorithm shows the rapidly deteriorating convergence performance. To solve this problem, this paper proposed the robust total minimum mean M-estimator normalized subband filter (TLMM-NSAF) algorithm. In addition, this paper also conducts a detailed theoretical performance analysis of the TLMM-NSAF algorithm and obtains the stable step size range and theoretical steady-state mean squared deviation (MSD) of the algorithm. To further improve the performance of the algorithm, we also propose a new variable step size (VSS) method of the algorithm. Finally, the robustness of our proposed algorithm and the consistency of theoretical and simulated values are verified by computer simulations of system identification and echo cancellation under different noise models.

Index Terms—errors-in-variables model, M-estimate, total least squares, subband adaptive filter, correlated input.

I. INTRODUCTION

Adaptive filtering has been widely used in many fields such as system identification and echo cancellation [1]. The classical normalized least mean square (NLMS) algorithm is universally adopted due to its efficiency and simplicity [2]. Nevertheless, when the input signal is a correlated input signal, the convergence of the NLMS algorithm becomes poor. The Affine Projection Algorithm (APA) can solve this problem [3], but it is computationally expensive [4]. In [7], Lee et al. proposed the normalized subband adaptive filter (NSAF) algorithm, which converges better than the NLMS algorithm under correlated inputs without significantly increasing the computational complexity.

However, the above traditional adaptive filtering algorithms only assume that the output noise is polluted. Under the EIV model where both the input and output signals have noise

interference, the convergence performance of the traditional adaptive filtering algorithm will deteriorate. In the past, the bias-compensated (BC) method was often used under the EIV model, which introduced bias compensation vectors to compensate for estimation errors caused by noise in the input signal. A number of adaptive filtering algorithms utilizing the bias-compensated method are already proposed [14]–[16].

Different from BC method, The total least squares (TLS) has good convergence performance when dealing with Errors-in-variables (EIV) models. Reference [9] extended the TLS algorithm to subbands and proposed the TLS-NSAF algorithm, which showed good performance under the EIV model. Unfortunately, the performance of the TLS-NSAF algorithm deteriorates severely when disturbed by impulse noise. Although the impulse noise is short in duration, it has a large amplitude and causes the algorithm's convergence behavior to fluctuate wildly. In order to obtain stable convergence in impulse noise, a sign algorithm was first proposed by minimizing the absolute value of the error signal, but the convergence speed is slow [33][34]. In addition to sign algorithm, The M-estimator function (MF) has the ability to distinguish outliers, and excellent performance against impulse noise, so it is used by many adaptive algorithms to improve robustness to impulse noise [10]–[12], [23].

Aiming at the problem that the performance of TLS-NSAF algorithm is seriously degraded when it suffers from impulse noise, this paper proposes a robust total minimum mean M-estimated normalized subband filter (TLMM-NSAF) algorithm. The algorithm shows good performance under the EIV model and is robust to impulse noise. More importantly, a detailed theoretical analysis is provided for the TLMM-NSAF algorithm. To further improve the performance of the algorithm, we used the existing VSS strategy [18][29][35] to improve the traditional convex combination method [30], and proposed a new VSS method. Finally, the simulations of system identification and echo cancellation under different noise models verify the robustness of our proposed algorithm and the consistency of theoretical and simulated values. The following are the main contributions of this paper.

- 1) The proposed TLMM-NSAF algorithm shows good performance under the EIV model where the input signal is a correlated input signal and is disturbed by impulse noise.
- 2) The local stability, computational complexity and steady-state MSD of the TLMM-NSAF algorithm under impulse noise are analyzed. The analytical results are supported by simulations.
- 3) In order to improve the performance of the

This work was partially supported by National Natural Science Foundation of China (grant: 62171388, 61871461, 61571374), Fundamental Research Funds for the Central Universities (grant: 2682021ZTPY091).

Haiquan Zhao, Zian Cao and Yida Chen are with the Key Laboratory of Magnetic Suspension Technology and Maglev Vehicle, Ministry of Education, and the School of Electrical Engineering, Southwest Jiaotong University, Chengdu, 610031, China. (e-mail: hqzhao_swjtu@126.com; ziancao_swjtu@126.com; yidachen_swjtu@126.com).

Corresponding author: Haiquan Zhao.

TLMM-NSAF algorithm, the existing VSS strategy is improved, and a Variable step convex combination total least squares normalized subband adaptive filter algorithm (VSS-CTLMM-NSAF) is proposed.

4) The proposed algorithms are validated in simulations for system identification and acoustic echo cancellation.

The remaining part of this paper is organized as follows. Section II introduces the subband structure of the input signal contaminated by noise and reviews the EIV model and the TLS-NSAF algorithm. Section III deduces the TLMM-NSAF algorithm in detail. Section IV analyzes the local stability of the algorithm under impulse noise interference, and obtains the step size range to ensure the stability of the algorithm. Section V calculates the steady-state MSD of the TLMM-NSAF algorithm. Section VI proposed a new VSS method. The computational complexity of different algorithms is analyzed in Section VII. Section VIII presents the simulation results. The last section gives the conclusion.

II. BRIEF REVIEW

A. EIV model and subband adaptive filter (SAF) structure

There exists a linear system which is expressed as:

$$d(z) = \mathbf{w}_0^T \mathbf{x}(z), \quad (1)$$

where $\mathbf{w}_0 \in \mathbb{R}^{L \times 1}$ is unknown weight vector, $\mathbf{x}(z) = [x(z), \dots, x(z-L+1)]^T \in \mathbb{R}^{L \times 1}$ and $d(z) \in \mathbb{R}$ are input vector and corresponding output signal respectively.

In the EIV model, both the input and output signals are disturbed by noise, and can be described as:

$$\tilde{\mathbf{x}}(z) = \mathbf{x}(z) + \mathbf{u}(z), \quad (2)$$

$$\tilde{d}(z) = d(z) + v(z), \quad (3)$$

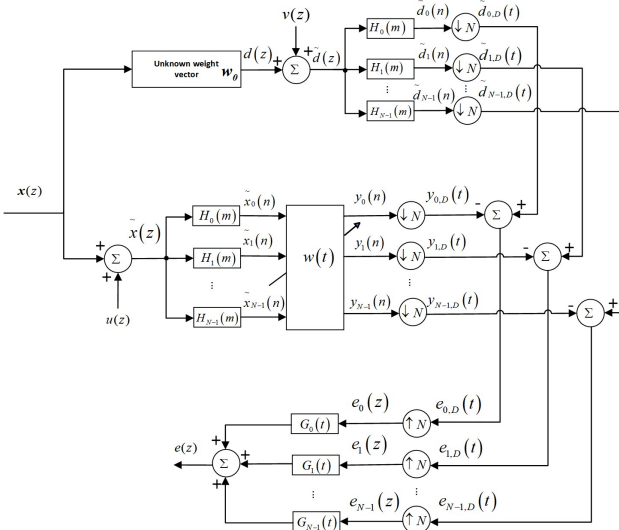


Fig. 1. Subband adaptive filter under EIV model

where $\mathbf{u}(z) \in \mathbb{R}^{L \times 1}$ and $v(z) \in \mathbb{R}$ are the input and output noise signals, of which the variance is σ_u^2 and σ_v^2 , respectively.

The subband adaptive filter structure under the EIV model is given by Fig. 1: The analysis filter $H_i(m)$, $i = 0, \dots, N-1$ decomposes the input signal $\tilde{\mathbf{x}}_i(z)$ and the desired

signal $\tilde{d}_i(z)$ proportionally to obtain the subband input signal $\tilde{\mathbf{x}}_i(z)$ and the subband desired signal $\tilde{d}_i(z)$. $y_i(z)$ is the subband output signal. Strict downsampling of subband signals $\tilde{d}_i(z)$ and $y_i(z)$ can generate signals $\tilde{d}_{i,D}(t)$ and $y_{i,D}(t)$ with lower sampling rates. The subband error signal is obtained by

$$e_{i,D}(t) = \tilde{d}_{i,D}(t) - y_{i,D}(t) = \tilde{d}_{i,D}(t) - \tilde{\mathbf{x}}_i^T(t) \mathbf{w}(t), \quad (4)$$

where the subband input signal and the weight vector are expressed as

$$\tilde{\mathbf{x}}_i(t) = [\tilde{x}_i(tN), \tilde{x}_i(tN-1), \dots, \tilde{x}_i(tN-L+1)]^T \in \mathbb{R}^{L \times 1}, \quad \text{and}$$

$\mathbf{w}(t) = [w_0(t), w_1(t), \dots, w_{L-1}(t)]^T \in \mathbb{R}^{L \times 1}$. The index of the decimated sequence is defined as variable t in this paper.

B. TLS-NSAF algorithm

In [9], the author applies the TLS method to subband adaptive filtering and proposes the TLS-NSAF algorithm. To minimize the interference of input noise and output noise to the system, the TLS method in a single subband can be described by [17]

$$\min_{\mathbf{w}} J_{i,z}(\mathbf{w}) = \sum_{j=1}^z \frac{(\tilde{d}_{i,D}(j) - \tilde{\mathbf{x}}_i^T(j) \mathbf{w})^2}{\|\mathbf{w}\|^2 + \theta_i}. \quad (5)$$

Where the ratio of the noise variance of the output signal to the input signal is $\theta_i = \sigma_{i,o}^2 / \sigma_{i,in}^2$, and in practice the values of $\sigma_{i,o}^2$ and $\sigma_{i,in}^2$ are often very close or the same [19].

Because the input data and the input and output noises are correlation ergodic processes, the time average in (5) is replaced with the expectation and obtain the following alternative cost function:

$$J_i(\mathbf{w}) = E \left[\frac{(\tilde{d}_{i,D}(t) - \tilde{\mathbf{x}}_i^T(t) \mathbf{w})^2}{\|\mathbf{w}\|^2 + \theta_i} \right] = E \left[\frac{e_{i,D}^2(t)}{\|\bar{\mathbf{w}}\|^2} \right]. \quad (6)$$

Where $\bar{\mathbf{w}} = [\mathbf{w}^T, -\sqrt{\theta_i}]^T$. Then, the cost function in the full-band filter is obtained as

$$J_{\text{TLS-NSAF}}(\mathbf{w}) = \sum_{i=0}^{N-1} E \left[\frac{e_{i,D}^2(t)}{\|\bar{\mathbf{w}}\|^2} \right]. \quad (7)$$

Adding the normalization term to $J_{\text{TLS-NSAF}}(\mathbf{w})$ in (9) because of the advantages of the multi-band-structured SAF (MSAF) [7], [8], [21]. Then the cost function of the TLS-NSAF algorithm is obtained as

$$J_{\text{TLS-NSAF}}(\mathbf{w}) = \sum_{i=0}^{N-1} E \left[\frac{e_{i,D}^2(t)}{\|\tilde{\mathbf{x}}_i(t)\|^2 \|\bar{\mathbf{w}}\|^2} \right]. \quad (8)$$

III. THE PROPOSED TLMM ALGORITHM

Inspired by the least mean M-estimate (LMM) algorithm [24], the TLMM-NSAF algorithm is proposed, which is derived based on the following cost function

$$J_{\text{TLMM-NSAF}}(\mathbf{w}) = \sum_{i=0}^{N-1} E \left[\frac{\rho(e_{i,D}(t))}{\|\tilde{\mathbf{x}}_i(t)\|^2 \|\bar{\mathbf{w}}\|^2} \right]. \quad (9)$$

where $\rho(\cdot)$ is the M-estimate function, which has been widely used in existing literatures [24-26], [20]. The modified Huber function is used as the M-estimate function due to its simplicity and efficiency

$$\rho(e_{i,D}(t)) = \begin{cases} \frac{e_{i,D}^2(t)}{2}, & |e_{i,D}(t)| < \xi_i \\ \frac{\xi_i^2 \|\bar{\mathbf{w}}\|^2}{2}, & |e_{i,D}(t)| \geq \xi_i \end{cases} \quad (10)$$

where ξ_i is the threshold parameter for controlling the suppression of impulse noise. In general, ξ_i is adjusted by $\xi_i = 2.576\hat{\sigma}_{e,i}(t)$ [25]. The robust estimator $\hat{\sigma}_{e,i}(n)$ can be obtained by

$$\hat{\sigma}_{e,i}^2(t) = \lambda_\sigma \hat{\sigma}_{e,i}^2(t-1) + k(1 - \lambda_\sigma) \text{med}(A_{e,i}(t))$$

where λ_σ is a forgetting factor and $0 < \lambda_\sigma < 1$. $k = 1.483(1 + 5/(N_w - 1))$ is the correction factor. The N_w is usually chosen between 5 and 9 [26]. $\text{med}(\cdot)$ is the median operator and $A_{e,i}(t) = [e_{i,D}^2(t), e_{i,D}^2(t-1), \dots, e_{i,D}^2(t - N_w + 1)]$. Using the gradient descent method, the gradient vector $\mathbf{g}_{TLMM-NSAF}(\mathbf{w})$ of $J_{TLMM-NSAF}(\mathbf{w})$ can be calculated as:

$$\mathbf{g}_{TLMM-NSAF}(\mathbf{w}) = \frac{\partial J_{TLMM-NSAF}}{\partial \mathbf{w}} = \begin{cases} -E \left[\sum_{i=0}^{N-1} \frac{\|\bar{\mathbf{w}}\|^2 e_{i,D}(t) \tilde{\mathbf{x}}_i(t) + e_{i,D}^2(t) \mathbf{w}}{\|\tilde{\mathbf{x}}_i(t)\|^2 \|\bar{\mathbf{w}}\|^4} \right] & |e_{i,D}(t)| < \xi_i \\ 0 & |e_{i,D}(t)| \geq \xi_i \end{cases} \quad (11)$$

Because the subband input power has the chi-square distribution under L degrees of freedom [13], (11) can be simplified as:

$$\mathbf{g}_{TLMM-NSAF}(\mathbf{w}) = \frac{\partial J_{TLMM-NSAF}}{\partial \mathbf{w}} = \begin{cases} -E \left[\sum_{i=0}^{N-1} \frac{\|\bar{\mathbf{w}}\|^2 e_{i,D}(t) \tilde{\mathbf{x}}_i(t) + e_{i,D}^2(t) \mathbf{w}}{(L-2)\sigma_{i,\bar{\mathbf{x}}}^2 \|\bar{\mathbf{w}}\|^4} \right] & |e_{i,D}(t)| < \xi_i \\ 0 & |e_{i,D}(t)| \geq \xi_i \end{cases} \quad (12)$$

After replacing the expected value with the instantaneous value, the instantaneous gradient vector can be further obtained:

$$\hat{\mathbf{g}}_{TLMM-NSAF}(\mathbf{w}) = \begin{cases} -\sum_{i=0}^{N-1} \frac{\|\bar{\mathbf{w}}\|^2 e_{i,D}(t) \tilde{\mathbf{x}}_i(t) + e_{i,D}^2(t) \mathbf{w}}{(L-2)\sigma_{i,\bar{\mathbf{x}}}^2 \|\bar{\mathbf{w}}\|^4} & |e_{i,D}(t)| < \xi_i \\ 0 & |e_{i,D}(t)| \geq \xi_i \end{cases} \quad (13)$$

Using (13), can obtain the weight vector update formula of the TLMM-NSAF algorithm as:

$$\begin{aligned} \mathbf{w}(t+1) &= \mathbf{w}(t) - \mu \hat{\mathbf{g}}_{TLMM-NSAF}(\mathbf{w}(t)) \\ &= \begin{cases} \mathbf{w}(t) + \mu \sum_{i=0}^{N-1} \frac{\|\bar{\mathbf{w}}(t)\|^2 e_{i,D}(t) \tilde{\mathbf{x}}_i(t) + e_{i,D}^2(t) \mathbf{w}(t)}{(L-2)\sigma_{i,\bar{\mathbf{x}}}^2 \|\bar{\mathbf{w}}(t)\|^4} & |e_{i,D}(t)| < \xi_i \\ \mathbf{w}(t) & |e_{i,D}(t)| \geq \xi_i \end{cases} \end{aligned} \quad (14)$$

It can be proved from (13) that the output error will be large due to the impulse noise, which will cause $|e_{i,D}(t)| \geq \xi_i$ so that the weight vector will not be updated at this time, thus effectively avoiding the interference of impulse noise.

The pseudo-code of the TLMM-NSAF algorithm is given in TABLE I.

TABLE I
THE PSEUDO-CODE OF THE TLMM-NSAF ALGORITHM.

Initialization: $\mathbf{w}(0) = \mathbf{0}$
Parameters: $\mu, N_w, \lambda_\sigma, k = 1.483(1 + 5/(N_w - 1))$
For $z = 0, 1, 2, \dots$
For $i = [0, N-1]$
$e_{i,D}(t) = \tilde{d}_{i,D}(t) - \tilde{\mathbf{x}}_i^T(t) \mathbf{w}(t)$
$A_{e,i}(t) = [e_{i,D}^2(t), e_{i,D}^2(t-1), \dots, e_{i,D}^2(t - N_w + 1)]$
$\hat{\sigma}_{e,i}^2(t) = \lambda_\sigma \hat{\sigma}_{e,i}^2(t-1) + k(1 - \lambda_\sigma) \text{med}(A_{e,i}(t))$
$\xi_i = 2.576 \hat{\sigma}_{e,i}(t)$
If $ e_{i,D}(t) < \xi_i$
$\mathbf{w}(t+1) = \mathbf{w}(t) + \mu \sum_{i=0}^{N-1} \frac{\ \bar{\mathbf{w}}(t)\ ^2 e_{i,D}(t) \tilde{\mathbf{x}}_i(t) + e_{i,D}^2(t) \mathbf{w}(t)}{(L-2)\sigma_{i,\bar{\mathbf{x}}}^2 \ \bar{\mathbf{w}}(t)\ ^4}$
else
$\mathbf{w}(t+1) = \mathbf{w}(t)$
End
End
End

IV. LOCAL STABILITY ANALYSIS

The local extreme points of the cost function $J_{TLMM-NSAF}(\mathbf{w})$ and the local stability of the TLMM-NSAF algorithm are analyzed in detail in this section, and the range of step sizes that the algorithm can converge stably is also determined.

To make the analysis tractable, the following common assumptions in adaptive filtering analysis are provided [1].

Assumption 1: The input noise vector $\mathbf{u}_i(t)$, the weight vector $\mathbf{w}(t)$, the input vector $\mathbf{x}_i(t)$ and the output noise $v_i(t)$ are independent mutually [1], [14], [15].

Assumption 2: The analysis filter bank is paraunitary [13], [15].

Assumption 3: When L is long, the fluctuation of $\|\tilde{\mathbf{x}}_i(t)\|^2$ from one time to the next is small enough [6], [13].

A. Local extreme point

It can be seen from equations (12)-(14) that when $|e_{i,D}(t)| \geq \xi_i$, the gradient vector $\hat{\mathbf{g}}_{TLMM-NSAF}(\mathbf{w}) = 0$, and the weight vector will not be updated at this time. Therefore, the following theoretical analysis only need consider the case of $|e_{i,D}(t)| < \xi_i$.

From formula (1), \mathbf{w}_0 is the ideal optimal weight vector and the value of the gradient vector $\hat{\mathbf{g}}_{TLMM-NSAF}(\mathbf{w})$ in (13) at \mathbf{w}_0 can be written as :

$$\mathbf{g}_{TLMM-NSAF}(\mathbf{w}_0) = -\sum_{i=0}^{N-1} \frac{\|\bar{\mathbf{w}}_0\|^2 E[e_{i,D}(t)\tilde{\mathbf{x}}_i(t)] + E[e_{i,D}^2(t)]\mathbf{w}_0}{(L-2)\sigma_{i,\tilde{x}}^2 \|\bar{\mathbf{w}}_0\|^4}. \quad (15)$$

The weight vector update formula in (14) also can be written as

$$\mathbf{w}(t+1) = \mathbf{w}(t) + \mu \sum_{i=0}^{N-1} \frac{\|\bar{\mathbf{w}}(t)\|^2 e_{i,D}(t)\tilde{\mathbf{x}}_i(t) + e_{i,D}^2(t)\mathbf{w}(t)}{(L-2)\sigma_{i,\tilde{x}}^2 \|\bar{\mathbf{w}}(t)\|^4}.$$

The error $e_{i,D}(t)$ at \mathbf{w}_0 can be get by

$$e_{i,D}(t) = \tilde{d}_{i,D}(t) - \mathbf{w}_0^T \tilde{\mathbf{x}}_i(t) = v_i(t) - \mathbf{w}_0^T \mathbf{u}_i(t). \quad (16)$$

Based on Assumption 1, the expectation in equation (15) can be calculated as:

$$E[e_{i,D}^2(t)] = E[v_i^2(t)] + E[(\mathbf{w}_0^T \mathbf{u}_i(t))^2] = \|\bar{\mathbf{w}}_0\|^2 \sigma_{i,in}^2 \quad (17)$$

and

$$\begin{aligned} E[e_{i,D}(t)\tilde{\mathbf{x}}_i(t)] \\ = E[(v_i(t) - \mathbf{w}_0^T \mathbf{u}_i(t))(\mathbf{x}_i(t) + \mathbf{u}_i(t))] = -\mathbf{w}_0 \sigma_{i,in}^2. \end{aligned} \quad (18)$$

Substituting (17) and (18) to (15), we can calculate $\mathbf{g}_{TLMM-NSAF}(\mathbf{w}_0) = 0$. So, \mathbf{w}_0 is the critical point of $J_{TLMM-NSAF}(\mathbf{w})$. To further prove that \mathbf{w}_0 is a local extreme point, it is necessary to calculate the Hessian matrix $\mathbf{H}_{TLMM-NSAF}(\mathbf{w})$ of $J_{TLMM-NSAF}(\mathbf{w})$.

By differentiating (12) with respect to \mathbf{w}^T , the Hessian matrix can be calculated as

$$\begin{aligned} \mathbf{H}_{TLMM-NSAF}(\mathbf{w}) &= \frac{\partial \mathbf{g}_{TLMM-NSAF}(\mathbf{w})}{\partial \mathbf{w}^T} = \frac{1}{\|\bar{\mathbf{w}}\|^2} \left[\sum_{i=0}^{N-1} \frac{E[\tilde{\mathbf{x}}_i(t)\tilde{\mathbf{x}}_i^T(t)]}{\sigma_{i,\tilde{x}}^2(L-2)} \mathbf{I} \right. \\ &\quad \left. - \sum_{i=0}^{N-1} \frac{E[e_{i,D}^2(t)]}{(L-2)\sigma_{i,\tilde{x}}^2 \|\bar{\mathbf{w}}\|^2} \mathbf{I} - \mathbf{g}_{TLMM-NSAF}(\mathbf{w})\mathbf{w}^T - \mathbf{w}\mathbf{g}_{TLMM-NSAF}^T(\mathbf{w}) \right]. \end{aligned} \quad (19)$$

So the Hessian matrix at \mathbf{w}_0 is obtained as :

$$\mathbf{H}_{TLMM-NSAF}(\mathbf{w}_0) = \frac{1}{\|\bar{\mathbf{w}}_0\|^2} \left\{ \sum_{i=0}^{N-1} \left[\gamma_i \mathbf{I} - \frac{\sigma_{i,in}^2 \mathbf{I}}{\sigma_{i,\tilde{x}}^2(L-2)} \right] \right\}, \quad (20)$$

where $\gamma_i \mathbf{I} \approx \frac{E[\tilde{\mathbf{x}}_i(t)\tilde{\mathbf{x}}_i^T(t)]}{E[\|\tilde{\mathbf{x}}_i(t)\|^2]}$ and γ_i is only influenced by the

correlatedness of the input signal and affects the convergence rate. When the number of subbands is sufficiently large or the original input signal is the white signal, the subband input signal is a white signal[9]. In this case $\gamma_i \approx \frac{1}{L}$. When the input

signal is the relevant input signal, γ_i is determined as the average value of α_i and $\frac{1}{L}$ for the correlated input signal.

Where α_i means the minimum eigenvalue of the covariance matrix of the i th subband input. The content of γ_i is covered in detail in [27].

because of the variance of the input noise is smaller than the variance of the input signal in a noisy subband input signal, so it can be obtained:

$$\sigma_{i,\tilde{x}}^2 > \sigma_{i,in}^2. \quad (21)$$

To prove that \mathbf{w}_0 is a local minimum point, it is also necessary to prove that the Hessian matrix $\mathbf{H}_{TLMM-NSAF}(\mathbf{w})$ is positive definite. According to (20), when the following conditions are satisfied, the $\mathbf{H}_{TLMM-NSAF}(\mathbf{w})$ is positive definite.

$$(L-2) \frac{\sigma_{i,\tilde{x}}^2}{\sigma_{i,in}^2} > \frac{1}{\gamma_i}. \quad (22)$$

Because of the filter order L is much larger than 2 and $\frac{\sigma_{i,\tilde{x}}^2}{\sigma_{i,in}^2} > 1$ can be known from equation (21), so the condition of equation (22) is satisfied and it can be proved that the $\mathbf{H}_{TLMM-NSAF}(\mathbf{w})$ is a positive definite matrix, and \mathbf{w}_0 is a local minimum point.

B. Local mean stability

The local stability of the TLMM-NSAF algorithm was analyzed in this section. For convenient analysis

that converges to the vicinity of \mathbf{w}_0 after a sufficient number of iterations. Since the instantaneous value is used to replace the expected value (13), it will cause a gradient error, which is defined as:

$$\mathbf{r}(\mathbf{w}(t)) \triangleq \hat{\mathbf{g}}_{TLMM-NSAF}(\mathbf{w}(t)) - \mathbf{g}_{TLMM-NSAF}(\mathbf{w}(t)). \quad (23)$$

Substituting (23) into (14), the weight update can rewrite as

$$\mathbf{w}(t+1) = \mathbf{w}(t) - \mu \mathbf{g}_{TLMM-NSAF}(\mathbf{w}(t)) - \mu \mathbf{r}(\mathbf{w}(t)). \quad (24)$$

By subtracting \mathbf{w}_0 from both sides of equation (24) at the same time, the update formula for the weight error vector can be obtained:

$$\tilde{\mathbf{w}}(t+1) = \tilde{\mathbf{w}}(t) + \mu \mathbf{g}_{TLMM-NSAF}(\mathbf{w}(t)) + \mu \mathbf{r}(\mathbf{w}(t)). \quad (25)$$

Where $\tilde{\mathbf{w}}(t) \stackrel{\text{def}}{=} \mathbf{w}_0 - \mathbf{w}(t)$. since $J_{TLMM-NSAF}(\mathbf{w})$ is twice continuously differentiable near the straight line between \mathbf{w}_0 and $\mathbf{w}(t)$ [17]-[18], so employing Theorem 1.2.1 in the literature [22] the gradient can be calculated as

$$\begin{aligned} \mathbf{g}_{TLMM-NSAF}(\mathbf{w}(t)) \\ = \mathbf{g}_{TLMM-NSAF}(\mathbf{w}_0) - \left[\int_0^1 \mathbf{H}_{TLMM-NSAF}(\mathbf{w}_0 - T\tilde{\mathbf{w}}(t)) dT \right] \tilde{\mathbf{w}}(t) \\ \approx \left[\int_0^1 \mathbf{H}_{TLMM-NSAF}(\mathbf{w}_0) dT \right] \tilde{\mathbf{w}}(t) \\ = -\mathbf{H}_{TLMM-NSAF}(\mathbf{w}_0) \tilde{\mathbf{w}}(t) \end{aligned} \quad (26)$$

Since $\tilde{\mathbf{w}}(t)$ is very small near the expected solution \mathbf{w}_0 , an

approximation $\mathbf{w}_0 - T\tilde{\mathbf{w}}(t) \approx \mathbf{w}_0$ can be obtained.

In addition, an approximation of the gradient error vector in steady state can also be written as

$$\mathbf{r}(\mathbf{w}(t)) \approx \mathbf{r}(\mathbf{w}_0) = \hat{\mathbf{g}}_{\text{TLMM-NSAF}}(\mathbf{w}_0). \quad (27)$$

Substituting (26) and (27) into (25) to get

$$\begin{aligned} \tilde{\mathbf{w}}(t+1) &\approx \tilde{\mathbf{w}}(t) - \mu \mathbf{H}_{\text{TLMM-NSAF}}(\mathbf{w}_0) \tilde{\mathbf{w}}(t) + \mu \mathbf{r}(\mathbf{w}_0) \\ &\approx (\mathbf{I} - \mu \mathbf{H}_{\text{TLMM-NSAF}}(\mathbf{w}_0)) \tilde{\mathbf{w}}(t) + \mu \mathbf{r}(\mathbf{w}_0) \end{aligned} \quad (28)$$

Next, take the expectation on both sides of (28):

$$E[\tilde{\mathbf{w}}(t+1)] = (\mathbf{I} - \mu \mathbf{H}_{\text{TLMM-NSAF}}(\mathbf{w}_0)) E[\tilde{\mathbf{w}}(t)]. \quad (29)$$

Based on (29), the size of all eigenvalues of the matrix $\mathbf{I} - \mu \mathbf{H}_{\text{TLMM-NSAF}}(\mathbf{w}_0)$ needs to be less than 1 to ensure local convergence in the sense of the mean, so it can be described as:

$$|1 - \mu \lambda_{\max}\{\mathbf{H}_{\text{TLMM-NSAF}}(\mathbf{w}_0)\}| < 1. \quad (30)$$

Where $\lambda_{\max}\{\mathbf{A}\}$ represents the largest eigenvalue of matrix \mathbf{A} .

After substituting equation (20) into equation (30), the step size for stable convergence of the TLMM-NSAF algorithm is obtained as

$$0 < \mu < \frac{2}{\lambda_{\max}\left\{\frac{1}{\|\tilde{\mathbf{w}}_0\|^2} \left[\sum_{i=0}^{N-1} \gamma_i \mathbf{I} - \sum_{i=0}^{N-1} \frac{\sigma_{i,\text{in}}^2 \mathbf{I}}{\sigma_{i,\tilde{x}}^2 (L-2)} \right] \right\}}. \quad (31)$$

However, the following analysis is also required to ensure the stable convergence of the TLMM-NSAF algorithm:

By subtracting \mathbf{w}_0 (14) from both sides of the equation, the update formula of the weight error vector can be rewritten as:

$$\tilde{\mathbf{w}}(t+1) = \tilde{\mathbf{w}}(t) - \mu \hat{\mathbf{g}}_{\text{TLMM-NSAF}}(\mathbf{w}(t)). \quad (32)$$

Take the squared Euclidean norm of both sides of (32) and expected value, according to the definition of MSD, the following equation can be obtained:

$$\begin{aligned} \text{MSD}(t+1) &= \text{MSD}(t) - 2\mu E[\tilde{\mathbf{w}}(t)^T \hat{\mathbf{g}}_{\text{TLMM-NSAF}}(\mathbf{w}(t))] \\ &\quad + \mu^2 E[\hat{\mathbf{g}}_{\text{TLMM-NSAF}}(\mathbf{w}(t))^T \hat{\mathbf{g}}_{\text{TLMM-NSAF}}(\mathbf{w}(t))] \end{aligned} \quad (33)$$

and $\text{MSD}(z)$ in (33) is defined as $\text{MSD}(t) \stackrel{\text{def}}{=} E[\|\tilde{\mathbf{w}}(t)\|^2]$. For ensure the stable convergence of the TLMM-NSAF algorithm, it is necessary to satisfy

$$\text{MSD}(t+1) - \text{MSD}(t) < 0. \quad (34)$$

Substituting (34) into (33) yields the range of step size μ as:

$$0 < \mu < \frac{2E[\tilde{\mathbf{w}}(t)^T \hat{\mathbf{g}}_{\text{TLMM-NSAF}}(\mathbf{w}(t))]}{E[\hat{\mathbf{g}}_{\text{TLMM-NSAF}}(\mathbf{w}(t))^T \hat{\mathbf{g}}_{\text{TLMM-NSAF}}(\mathbf{w}(t))]}. \quad (35)$$

The paper [7] states that, consider the situation where the disturbance is negligible, the undisturbed error signal $\mathbf{w}_0^T \tilde{x}_i(t) - \mathbf{w}^T(t) \tilde{x}_i(t)$ is equal to the decimated subband error signal $e_{i,D}(t)$ and when the algorithm iterates enough, $\mathbf{w}(t) \approx \mathbf{w}_0$. So (35) can be simplified to

$$0 < \mu < 2(\|\mathbf{w}_0\|^2 + \theta_i) \quad (36)$$

Appendix A gives a detailed derivation of (36). Combining (32) and (33), the range of step sizes that make the algorithm stable can be obtained as:

$$0 < \mu < \min\left(2(\|\mathbf{w}_0\|^2 + \theta_i), \frac{2}{\lambda_{\max}\{\mathbf{H}_{\text{TLMM-NSAF}}(\mathbf{w}_0)\}}\right)$$

(37)

V. STEADY-STATE MEAN-SQUARE PERFORMANCE ANALYSIS

In (13), the steady-state MSD of the algorithm converges to a non-zero steady-state value because of the presence of the gradient error $\mathbf{r}(\mathbf{w}(t))$ (see Section IV above). This section uses an energy conservation method to predict this steady-state MSD.

Taking the square of the weighted Euclidean norm on both sides of Equation (25), and calculating the expectation of each term, and get:

$$E[\|\tilde{\mathbf{w}}(t+1)\|_\Lambda^2] \approx E[\|\tilde{\mathbf{w}}(t)\|_\Lambda^2] + \mu^2 E[\|\mathbf{r}(\mathbf{w}_0)\|_\Lambda^2]. \quad (38)$$

Λ is a non-negative definite weighting matrix and $\Theta = [\mathbf{I} - \mu \mathbf{H}_{\text{TLMM-NSAF}}(\mathbf{w})] \Lambda [\mathbf{I} - \mu \mathbf{H}_{\text{TLMM-NSAF}}(\mathbf{w})]$.

Furthermore, we define the square criterion of the weighted Euclidean norm of the vector \mathbf{s} as $\|\mathbf{s}\|_\Lambda^2 \stackrel{\text{def}}{=} \mathbf{s}^T \mathbf{A} \mathbf{s}$, where \mathbf{A} is the weighting matrix.

The analysis that follows uses the properties of matrices, vectorization operations, and the Kronecker product [28]:

$$\text{tr}\{\mathbf{X}^T \mathbf{Y}\} = \text{vec}\{\mathbf{Y}\}^T \text{vec}\{\mathbf{X}\},$$

$$\text{vec}\{\mathbf{XYZ}\} = (\mathbf{Z}^T \otimes \mathbf{X}) \text{vec}\{\mathbf{Y}\}.$$

Where \mathbf{X} , \mathbf{Y} , \mathbf{Z} are all matrices, \otimes is the Kronecker product and $\text{vec}\{\cdot\}$ is the vectorization operator that stacks the columns of its matrix argument into a single column vector.

In fact, matrix Λ is symmetric and deterministic. Applying the above two properties allows the following simplification operations:

$$\begin{aligned} E[\|\mathbf{r}(\mathbf{w}_0)\|_\Lambda^2] &= E[\text{tr}\{\Lambda \mathbf{r}(\mathbf{w}_0) \mathbf{r}(\mathbf{w}_0)^T\}] \\ &= \text{tr}\{E[\Lambda E[\mathbf{r}(\mathbf{w}_0) \mathbf{r}(\mathbf{w}_0)^T]]\} \\ &= \text{tr}\{\Lambda \mathbf{M}\} \\ &= \text{vec}\{\mathbf{M}\}^T \text{vec}\{\Lambda\} \\ &\stackrel{\text{def}}{=} \mathbf{m}^T \mathbf{n} \end{aligned} \quad (39)$$

where $\mathbf{m} \stackrel{\text{def}}{=} \text{vec}\{\mathbf{M}\}$, $\mathbf{n} \stackrel{\text{def}}{=} \text{vec}\{\Lambda\}$,

$$\begin{aligned} \mathbf{M} &= E[\mathbf{r}(\mathbf{w}_0) \mathbf{r}(\mathbf{w}_0)^T] \\ &= \sum_{i=0}^{N-1} \frac{\sigma_{i,\text{in}}^2}{\|\tilde{\mathbf{w}}_0\| (L-4) \sigma_{i,\tilde{x}}^2} \mathbf{I} - \sum_{i=0}^{N-1} \frac{1}{\|\tilde{\mathbf{w}}_0\|^4} \frac{3\sigma_{i,\tilde{x}}^4}{(L-2)(L-4)\sigma_{i,\tilde{x}}^4} \mathbf{w}_0 \mathbf{w}_0^T \end{aligned} \quad (40)$$

and

$$\begin{aligned} \text{vec}\{\Theta\} &= \text{vec}\{[\mathbf{I} - \mu \mathbf{H}_{\text{TLMM-NSAF}}(\mathbf{w})] \Lambda [\mathbf{I} - \mu \mathbf{H}_{\text{TLMM-NSAF}}(\mathbf{w})]\} \\ &= ([\mathbf{I} - \mu \mathbf{H}_{\text{TLMM-NSAF}}(\mathbf{w})] \otimes [\mathbf{I} - \mu \mathbf{H}_{\text{TLMM-NSAF}}(\mathbf{w})]) \text{vec}\{\Lambda\} \\ &\stackrel{\text{def}}{=} \mathbf{P} \mathbf{n}. \end{aligned} \quad (41)$$

Appendix B gives a detailed derivation of (40).

By substituting formulas (39) and (40) into formula (38), the following mean square relationship can be obtained:

$$E[\|\tilde{\mathbf{w}}(t+1)\|_n^2] \approx E[\|\tilde{\mathbf{w}}(t)\|_{P_n}^2] + \mu^2 \mathbf{m}^T \mathbf{n}. \quad (42)$$

According to the literature [1], [17], if the matrix \mathbf{P} is stable, the equation (42) can be guaranteed to converge to the steady state. Therefore, when the step size μ of the selected algorithm satisfies the formula (35), the matrix \mathbf{P} is stable. At this time, the mean and the mean square stability of the TLMM-NSAF algorithm can be satisfied.

When the algorithm iterates enough times, equation (42) can be rewritten as:

$$E[\|\tilde{\mathbf{w}}(\infty)\|_n^2] \approx E[\|\tilde{\mathbf{w}}(\infty)\|_{P_n}^2] + \mu^2 \mathbf{m}^T \mathbf{n}. \quad (43)$$

Then, we set \mathbf{n} to $(\mathbf{I} - \mathbf{P})^{-1} \text{vec}\{\mathbf{I}\}$ and get the steady-state MSD of the TLMM-NSAF algorithm as:

$$E[\|\tilde{\mathbf{w}}(\infty)\|_n^2] \approx \mu^2 \mathbf{m}^T (\mathbf{I} - \mathbf{P})^{-1} \text{vec}\{\mathbf{I}\}. \quad (44)$$

VI. THE VARIABLE STEP-SIZE STRATEGIES

Convex combination schemes of the VSS method [29] [18] and two independently operating filters [30] have been proposed in the existing literature. It is used to solve the problem that the fixed step size of the adaptive filtering algorithm cannot balance fast convergence and low steady-state estimation. This section combines the advantages of VSS with a convex combination scheme, and propose an improved variable stride strategy. The specific strategies are as follows:

$$\mathbf{w}(t) = \lambda(t) \mathbf{w}_1(t) + (1 - \lambda(t)) \mathbf{w}_2(t) \quad (45)$$

where $\mathbf{w}_1(t)$ and $\mathbf{w}_2(t)$ are two component filter weights, $\lambda(t)$ is a mixing parameter, and the overall filter weight $\mathbf{w}(t)$ is obtained by combining $\mathbf{w}_1(t)$ and $\mathbf{w}_2(t)$ through $\lambda(t)$. $\mathbf{w}_1(t)$ can be obtained by

$$\begin{aligned} \mathbf{w}_1(t+1) &= \mathbf{w}_1(t) - \mu_{\text{vss}}(t) \hat{\mathbf{g}}_{\text{TLMM-NSAF}}(\mathbf{w}_1(t)) \\ &= \begin{cases} \mathbf{w}_1(t) + \mu_{\text{vss}}(t) \sum_{i=0}^{N-1} \frac{\|\bar{\mathbf{w}}_1(t)\|^2 e_{i,D}(t) \tilde{\mathbf{x}}_i(t) + e_{i,D}^2(t) \mathbf{w}_1(t)}{(L-2)\sigma_{i,\tilde{\mathbf{x}}}^2 \|\bar{\mathbf{w}}_1(t)\|^4} & |e_{i,D}(t)| < \xi_i \\ \mathbf{w}_1(t) & |e_{i,D}(t)| \geq \xi_i \end{cases} \end{aligned} \quad (46)$$

$\mathbf{w}_2(t)$ can be obtained by

$$\begin{aligned} \mathbf{w}_2(t+1) &= \mathbf{w}_2(t) - \mu_2(t) \hat{\mathbf{g}}_{\text{TLMM-NSAF}}(\mathbf{w}_2(t)) \\ &= \begin{cases} \mathbf{w}_2(t) + \mu_2(t) \sum_{i=0}^{N-1} \frac{\|\bar{\mathbf{w}}_2(t)\|^2 e_{i,D}(t) \tilde{\mathbf{x}}_i(t) + e_{i,D}^2(t) \mathbf{w}_2(t)}{(L-2)\sigma_{i,\tilde{\mathbf{x}}}^2 \|\bar{\mathbf{w}}_2(t)\|^4} & |e_{i,D}(t)| < \xi_i \\ \mathbf{w}_2(t) & |e_{i,D}(t)| \geq \xi_i \end{cases} \end{aligned} \quad (47)$$

and

$$\mu_{\text{vss}}(t+1) = \begin{cases} \alpha \mu_{\text{vss}}(t) + \beta \sum_{i=0}^{N-1} e_{i,D}^2(t) & |e_{i,D}(t)| < \xi_i \\ \mu_{\text{vss}}(t) & |e_{i,D}(t)| \geq \xi_i \end{cases} \quad (48)$$

where $0 < \alpha < 1, \beta > 0$, $\mu_2(t)$ is a fixed small constant. Considering the stability of the algorithm and the required

tracking capability, we need to set a range for the step size $\mu_{\text{vss}}(t)$:

$$\mu_{\text{vss}}(t+1) = \begin{cases} \mu_{\max}, & \mu(t+1) > \mu_{\max} \\ \mu_{\text{vss}}(t+1), & \text{otherwise} \\ \mu_{\min}, & \mu(t+1) < \mu_{\min} \end{cases} \quad (49)$$

where μ_{\max} and μ_{\min} are the upper and lower bounds of the variable step size, respectively. The subband output signals of the overall filter are expressed as

$$y_{i,D}(t) = \lambda(t) y_{i,D,1}(t) + (1 - \lambda(t)) y_{i,D,2}(t) \text{ for } i \in [0, N-1]$$

where $y_{i,D,1}(t)$ and $y_{i,D,2}(t)$ denote the subband output signals of both component filters, respectively, which are given by

$$y_{i,D,1}(t) = \tilde{\mathbf{x}}_i^T(t) \mathbf{w}_1(t) \text{ and } y_{i,D,2}(t) = \tilde{\mathbf{x}}_i^T(t) \mathbf{w}_2(t).$$

Then, the overall subband error signals can be given by

$$e_{i,D}(t) = d_{i,D}(t) - y_{i,D}(t). \quad (50)$$

Evidently, the most critical problem of convex combination is how to adjust the mixing parameter $\lambda(t)$, which can be obtained by the following formula:

$$\lambda(t) = \frac{1}{1 + e^{-\alpha(t)}}. \quad (51)$$

where the auxiliary variable $\alpha(t)$ is updated by minimizing the cost function

$$J(t) = \sum_{i=0}^{N-1} e_{i,D}^2(t) \quad (52)$$

Taking the gradient of $J(t)$ with respect to $\alpha(t)$ gives:

$$\begin{aligned} \nabla J(t) &= \frac{\partial J(t)}{\partial \alpha(t)} \\ &= \lambda(t) [1 - \lambda(t)] \sum_{i=0}^{N-1} e_{i,D}(t) (y_{i,D,1}(t) - y_{i,D,2}(t)) \end{aligned} \quad (53)$$

Next, we adapt $\alpha(t)$ using the normalized gradient method, obtaining

$$\begin{aligned} \alpha(t+1) &= \alpha(t) - \mu_a \frac{\nabla J(t)}{\|\nabla J(t)\|} \\ &= \alpha(t) + \mu_a \text{sgn} \left[\sum_{i=0}^{N-1} e_{i,D}(t) (y_{i,D,1}(t) - y_{i,D,2}(t)) \right] \end{aligned} \quad (54)$$

where μ_a is a step size of $\alpha(t)$ and $\text{sgn}[\cdot]$ is the sign function.

Usually $\alpha(t)$ is restricted to the $[-a, a]$ range and the value of a is set to 4 [31].

In this way, the improved VSS-CTLMM-NSAF algorithm can not only further reduce the steady-state error, but also maintain a faster convergence rate during the entire algorithm convergence process. Section VIII gives simulation comparison of the variable step strategies total least squares normalized subband adaptive filter (VSS-TLMM-NSAF) algorithm, the convex combination total least squares normalized subband adaptive filter (CTLMM-NSAF) algorithm and the VSS-CTLMM-NSAF algorithm. Simulation results demonstrate the superiority of our proposed VSS

strategy. The pseudo-code of the VSS-CTLMM-NSAF algorithm is given in TABLE II.

TABLE II
THE PSEUDOCODE OF THE VSS-CTLMM-NSAF ALGORITHM.

Initialization: $w_1(0) = w_2(0) = 0, a^+ = 4, a(0) = 0$
Parameters: $k = 1.483(1 + 5/(N_w - 1)), j = 1, 2, \mu, N_w, \lambda_\sigma$
For $z = 0, 1, 2, \dots$ For $i = [0, N-1]$ $y_{j,i,D}(t) = \tilde{x}_i^T(t) w_j(t)$ $e_{j,i,D}(t) = \tilde{d}_{i,D}(t) - \tilde{x}_i^T(t) w_j(t)$ $y_{i,D}(t) = \lambda(t) y_{1,i,D}(t) + (1 - \lambda(t)) y_{2,i,D}(t)$ $e_{i,D}(t) = \lambda(t) e_{1,i,D}(t) + (1 - \lambda(t)) e_{2,i,D}(t)$ $A_{j,e,i}(t) = [e_{j,i,D}^2(t), e_{j,i,D}^2(t-1), \dots, e_{j,i,D}^2(t - N_w + 1)]$ $\hat{\sigma}_{j,e,i}^2(t) = \lambda_\sigma \hat{\sigma}_{j,e,i}^2(t-1) + k(1 - \lambda_\sigma) \text{med}(A_{j,e,i}(t))$ $\xi_{j,i} = 2.576 \hat{\sigma}_{j,e,i}(t)$ If $ e_{1,i,D}(t) < \xi_{1,i}$ $w_1(t+1) = w_1(t) + \mu_{\text{vss}}(t) \sum_{i=0}^{N-1} \frac{\ w_1(t)\ ^2 e_{1,i,D}(t) \tilde{x}_i(t) + e_{1,i,D}^2(t) w_1(t)}{(L-2)\sigma_{i,\tilde{x}}^2 \ w_1(t)\ ^4}$ $\mu_{\text{vss}}(t+1) = \alpha \mu_{\text{vss}}(t) + \beta \sum_{i=0}^{N-1} e_{i,D}^2(t)$ else $w_1(t+1) = w_1(t)$ $\mu_{\text{vss}}(t+1) = \mu_{\text{vss}}(t)$ End If $ e_{2,i,D}(t) < \xi_{2,i}$ $w_2(t+1) = w_2(t) + \mu_2 \sum_{i=0}^{N-1} \frac{\ w_2(t)\ ^2 e_{2,i,D}(t) \tilde{x}_i(t) + e_{2,i,D}^2(t) w_2(t)}{(L-2)\sigma_{i,\tilde{x}}^2 \ w_2(t)\ ^4}$ else $w_2(t+1) = w_2(t)$ End End Proposed combination scheme $\alpha(t+L) = \alpha(t) - \mu_a \text{sgn}\{\sum_{i=0}^{N-1} e_{i,D}(t)[y_{2,i,D}(t) - y_{1,i,D}(t)]\}$ $\alpha(t+L) = \min[\max(\alpha(t+L), -\alpha^+), \alpha^+]$ $\lambda(t+L) = \frac{1}{1 + e^{-\alpha(t+L)}}$ $w(t+L) = \lambda(t+L) w_1(t+L) + (1 - \lambda(t+L)) w_2(t+L)$ End

VII. COMPLEXITY ANALYSIS

The computational complexity of the TLMM-NSAF, NLMS, NSAF, VSS-TLMM-NSAF, CTLMM-NSAF, VSS-CTLMM-NSAF, M-NSAF and TLS-NSAF algorithms are presented in Table III. Where M expresses the length of the analysis filter; N means the number of subband filter; L denotes the length of the subband adaptive filter. As can be

seen from Table III, the computational complexity of the TLMM-NSAF algorithm is increased compared to the TLS-NSAF algorithm. Although the computational complexity increases, the magnitude of the increase is relatively small, and the proposed algorithm significantly enhances the robustness of the system against impulse noise interference. It can be seen that the increased computational complexity is acceptable and worthwhile. Compared with the VSS-TLMM-NSAF algorithm and CTLMM-NSAF algorithm, the computational complexity of the improved variable-step algorithm is also slightly increased. But the increased computational complexity is worth it, because the performance of the improved algorithm has been significantly improved.

TABLE III
COMPUTATIONAL COMPLEXITY

Algorithm	Multiplications	Additions	Divisions	Squarroot	Exponent
NLMS	$3L+1$	$3L-1$	1	0	0
NSAF	$3L+NM$ $+2M+2$	$3L+N(M-1)+$ $2(M-1)$	1	0	0
M-NSAF	$5L+NM+$ $2M+7$	$5L+N(M-1)+$ $2(M-1)+3$	2	0	0
TLS-NSAF	$6L+NM+$ $2M+3$	$5L+N(M-1)+$ $2(M-1)$	3	0	0
TLMM-NSAF	$6L+N(N_w+5)$ $+NM+2M+3$	$5L+N(M+3)+$ $2(M-1)$	4	1	0
VSS-TLMM-NSAF	$6L+N(N_w+8)$ $+NM+2M+3$	$5L+N(M+4)+$ $2(M-1)$	4	1	0
CTLMM-NSAF	$12L+2N(N_w+5)$ $+4NM+4M+11$	$10L+2N(M+3)+$ $4M+(M+4)/N$	$4+\frac{1}{N}$	1	$\frac{1}{N}$
VSS-CTLMM-NSAF	$12L+2N(N_w+8)$ $+4NM+4M+11$	$10L+2N(M+4)+$ $4M+(M+4)/N$	$4+\frac{1}{N}$	1	$\frac{1}{N}$

VIII. SIMULATIONS

This section verifies the previously proposed algorithm and theoretical results through simulations. All curves were obtained by averaging the results of 100 independent experiments, unless otherwise stated.

A. Number of different subbands

This subsection compares the performance of the TLMM-NSAF algorithm with different numbers of subbands. The unknown weight vector w_0 is generated with a uniform distribution from -0.5 to 0.5, $\|w_0\|^2 = 1$, ($L = 512$). The length of the subband adaptive filter is the same as the length of w_0 . The correlated input signal uses an Autoregressive (AR) model, which can be obtained by filtering a zero-mean Gaussian signal through $T_1(c) = 1/(1 - 0.8c^{-1})$ [16].

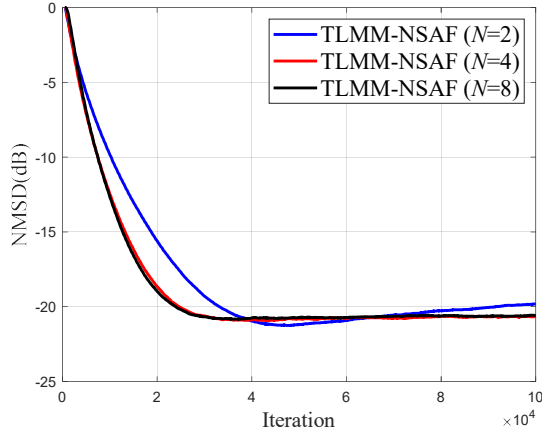


Fig. 2. TLMM-NSAF algorithm curves under different numbers of subband, without impulse noise
($\sigma_m^2 = 0.05, \sigma_o^2 = 0.05, \mu = 0.13$)

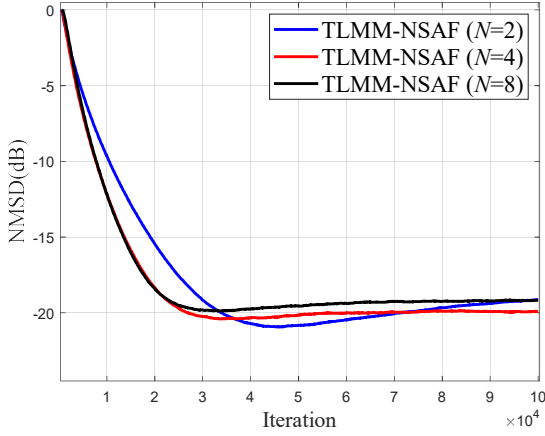


Fig. 3. TLMM-NSAF algorithm curves under different numbers of subband, contains impulse noise
($\sigma_m^2 = 0.05, \sigma_o^2 = 0.05, \mu = 0.13$)

For ease of comparison, we choose an appropriate step size parameter μ to ensure that the algorithm has the same convergence rate in early iterations. The algorithm performance evaluation index selects normalized mean square deviation (NMSD), which is defined as $NMSD = 10 \log_{10} (\|w(z) - w_0\|^2 / \|w_0\|^2)$.

From Figure 2 and Figure 3, it can be concluded that the more the number of subbands, the faster the algorithm convergence rate, but the NMSD will increase. When the number of subbands exceeds 4, the convergence speed of the algorithm does not increase significantly, and the computational complexity also increases. Therefore, the number of subbands is chosen to be 4 to obtain a suitable algorithm convergence speed and steady-state MSD.

B. Step size range

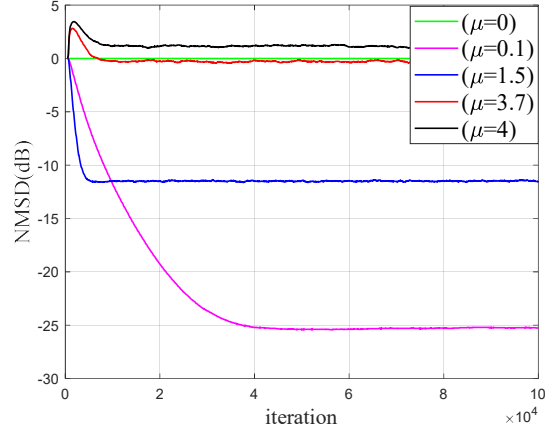


Fig. 4. TLMM-NSAF algorithm curve under different step lengths
($\sigma_m^2 = 0.05, \sigma_o^2 = 0.05, N = 4$)

From Figure 4, due to $\sigma_m^2 = 0.05, \sigma_o^2 = 0.05$, we can calculate the theoretical step size range of $[0, 4]$ to ensure the stability of the algorithm according to formula (37). It is worth mentioning that because of the use of some acceptable approximations, the range of step sizes that actually guarantees the stability of the algorithm will be slightly less than 4. The simulation results confirm our conclusion.

C. Comparison results of different algorithms under relevant inputs

It can be seen from Figure 5 and Figure 6 that the NSAF algorithm and the NLMS algorithm have poor convergence after being interfered by impulse noise, and the performance of the TLS-NSAF algorithm will be seriously deteriorated. The performance of M-NSAF algorithm and TLMM-NSAF algorithm is not disturbed by impulse noise. In addition, the simulation results show that the performance of the TLMM-NSAF algorithm is better than the M-NSAF algorithm. Furthermore, the performance of the VSS-CTLMM-NSAF algorithm is optimal with or without impulse noise.

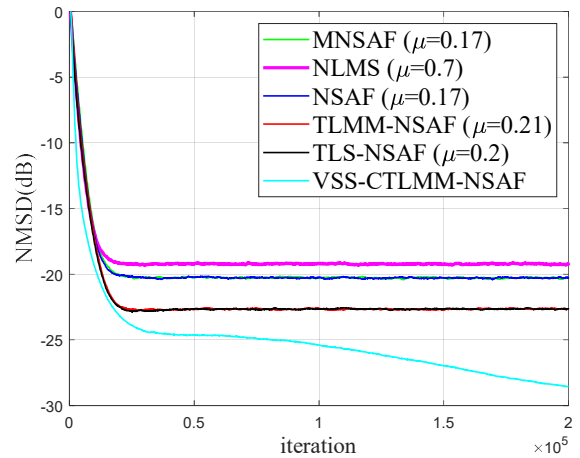


Fig. 5. Comparison curves of different algorithms under Gaussian noise $\sigma_m^2 = 0.05, \sigma_o^2 = 0.05, \theta_1 = 1$.

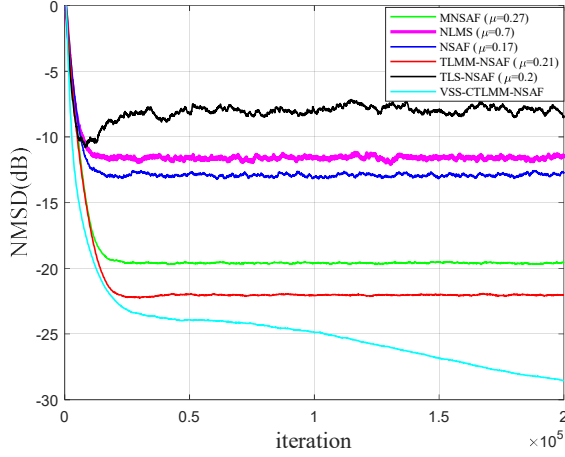


Fig. 6. Comparison of different algorithms under impulse noise

$$\sigma_{in}^2 = 0.05, \sigma_o^2 = 0.05, \theta_i = 1.$$

D. Comparison of variable step size algorithms under different strategies

As can be seen from Figure 7, the steady-state error of the CTLMM-NSAF algorithm is lower than that of the VSS-TLMM-NSAF algorithm, but the convergence speed is slower. The VSS-TLMM-NSAF algorithm converges speed is faster, but the steady-state error is slightly larger. Our proposed variable-step method combines the advantages of convex combinations and traditional variable-step strategies, resulting in faster algorithm convergence and smaller steady-state error. In contrast, the overall performance of the VSS-CTLMM-NSAF algorithm outperforms other algorithms.

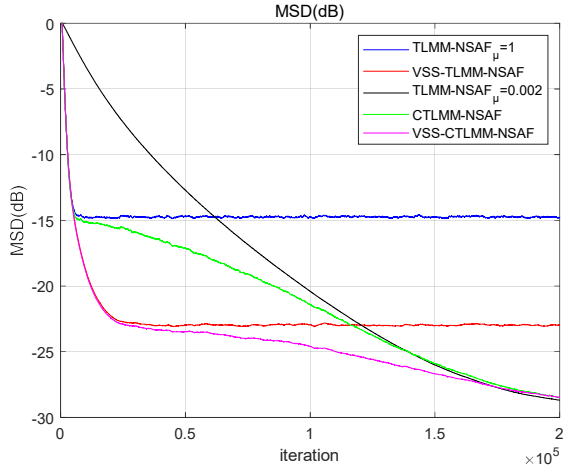


Fig. 7. Comparison of different algorithms under impulse noise

$$\sigma_{in}^2 = 0.05, \sigma_o^2 = 0.05, \theta_i = 1, \alpha = 0.99, \beta = 0.0058.$$

E. Algorithm theoretical performance verification

The theoretical performance of the TLMM-NSAF algorithm is verified in this subsection. Due to the limitation of computer simulation software performance, the dimension of the unknown system weight vector used is set to order 128.

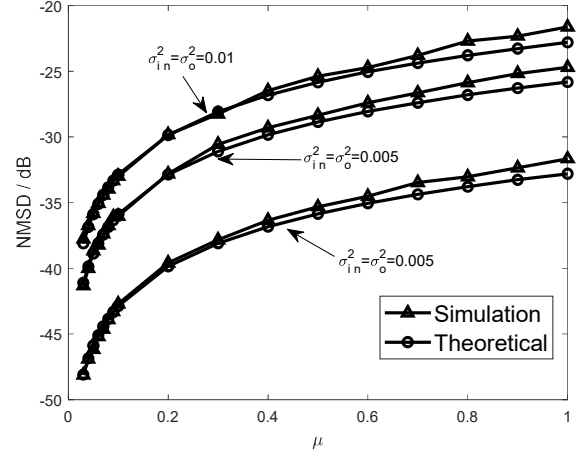


Fig. 8. Theoretical Steady-state MSD curves for different step lengths and noise variances (Gaussian input)

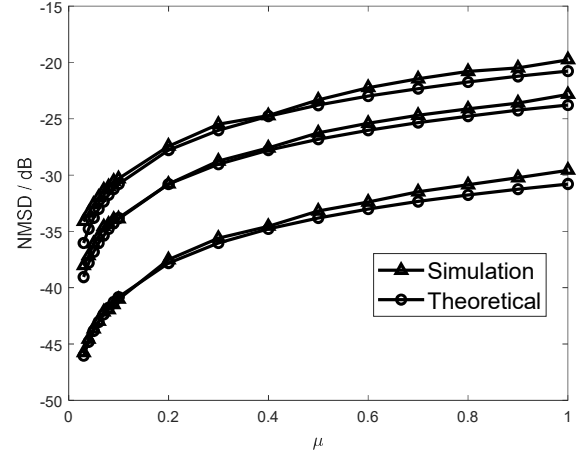


Fig. 9. Theoretical Steady-state MSD curves for different step lengths and noise variances (Related input)

The simulation results in the experiments are the average after 10 independent runs. The theoretical steady state value is calculated from Equation (38).

Figure 8 and Figure 9 are the simulation curves under Gaussian input and correlation input, respectively. From the simulation results it can be concluded that the theoretical curve of the proposed algorithm is basically consistent with the simulation curve under different variances. Although there are some minor differences, this is due to some assumptions and approximations made during the analysis, which are reasonable and acceptable. The comparison between the theoretical value curve and the simulation curve proves the accuracy of our analysis of the theoretical performance of the TLMM-NSAF algorithm.

F. Acoustic echo cancellation

In this subsection, the convergence performance of the TLMM-NSAF algorithm in echo cancellation applications under real speech input is verified.

Acoustic echo cancellation is commonly used in communication systems such as calls and video conferencing. Figure 10 shows the echo cancellation schematic.

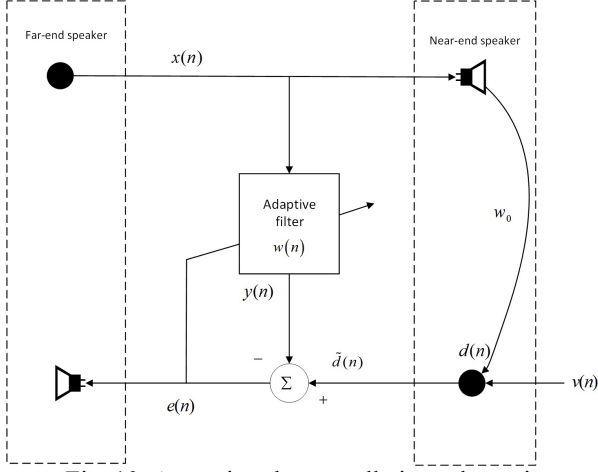


Fig. 10. Acoustic echo cancellation schematic

The application principle is as follows: $x(n)$ is the voice signal output by the far-end speaker, and also the input signal of the near-end speaker, w_0 is the pulse response of the echo channel, $d(n)$ is the echo signal generated by the input signal through the echo channel, and $v(n)$ is the background noise. According to the adaptive filtering and estimation algorithm, the weight parameter $w(n)$ is continuously adjusted, and the echo path channel w_0 is gradually fitted. Finally, the echo signal value $y(n)$ estimated by the adaptive filter is close to the real echo signal. The estimated echo signal is subtracted from the near-end speech signal, and the obtained output error signal $e(n) = \tilde{d}(n) - y(n)$ will have no echo, and then be sent to the far-end, so as to achieve the purpose of echo cancellation.

Figure 11 is the voice input signal, Figure 12 is the echo signal, Figure 13 is the simulation results of different algorithms under the input of speech signal without impulse noise, and Figure 14 is the simulation result of different algorithms under the input of speech signal with impulse noise. The simulation results show that the performance of the proposed TLMM-NSAF algorithm is comparable to that of the TLS-NSAF algorithm without the interference of impulse noise, and is superior to other algorithms. In the case of including impulse noise, the performance of other algorithms The deterioration is serious, while the TLMM-NSAF algorithm shows excellent robustness. In addition, the performance of the VSS-CTLMM-NSAF algorithm using the VSS strategy has a certain improvement in the convergence speed and convergence compared with the TLMM-NSAF algorithm.

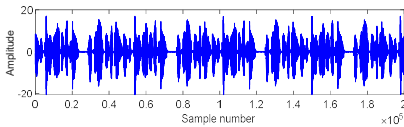


Fig. 11. Speech input signal

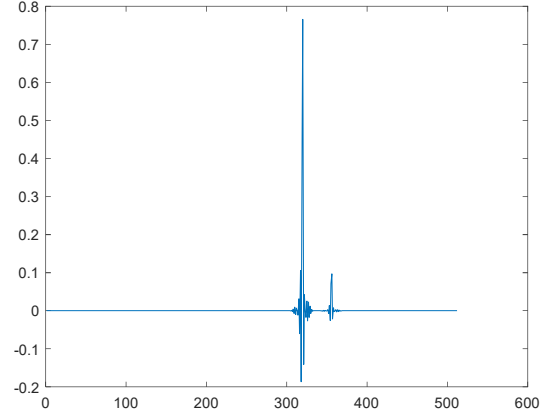


Fig. 12. Echo channel

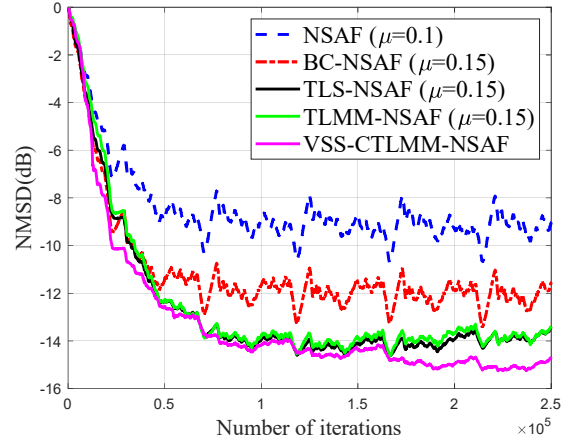


Fig. 13. Comparison of Steady-State MSD of different algorithms under speech input signal ($\sigma_m^2 = 0.05, \sigma_o^2 = 0.05, \theta_i = 1$, Gaussian noise)

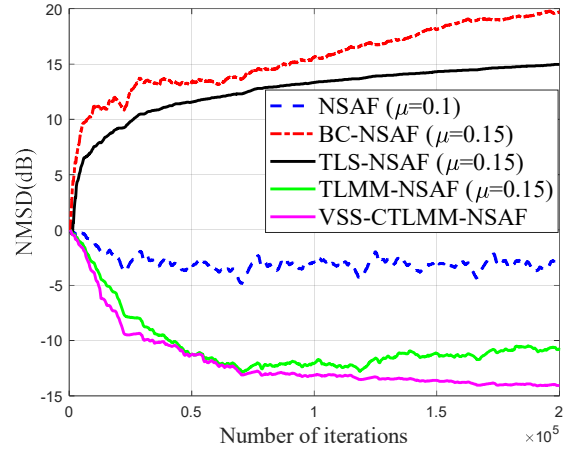


Fig. 14. Comparison of Steady-State MSD of different algorithms under speech input signal ($\sigma_m^2 = 0.05, \sigma_o^2 = 0.05, \theta_i = 1$, Contains impulse noise)

IX. CONCLUSION

In this work, the proposed TLMM-NSAF algorithm addresses the severe performance degradation of traditional

adaptive filtering algorithms under the EIV model disturbed by impulse noise. The detailed performance analysis of the TLMM-NSAF algorithm is carried out, and its analysis method also provides a good reference for the performance analysis of other sub-band adaptive filtering algorithms applying the TLS method in the future. In addition, in order to further improve the convergence speed and steady-state performance of the TLMM-NSAF algorithm, an improved VSS method is developed. Finally, we verify the convergence performance of the proposed TLMM-NSAF algorithm in system recognition and echo cancellation applications under real speech input, and demonstrate the superiority of our proposed algorithm by comparison with other adaptive filtering algorithms.

APPENDIX A

Section B of Chapter IV of this paper has been given: $\mathbf{h}^T \tilde{\mathbf{x}}_i(t) - \mathbf{w}^T(t) \tilde{\mathbf{x}}_i(t) = e_{i,D}(t)$ and when the algorithm iterates enough, $\mathbf{w}(t) \approx \mathbf{w}_0$. From this, (35) can be simplified to:

$$\frac{2E[\tilde{\mathbf{w}}(t)^T \hat{\mathbf{g}}_{TLMM-NSAF}(\mathbf{w}(t))]}{E[\hat{\mathbf{g}}_{TLMM-NSAF}(\mathbf{w}(t))^T \hat{\mathbf{g}}_{TLMM-NSAF}(\mathbf{w}(t))]} \approx \frac{2E\left[\frac{e_{i,D}^2}{\|\bar{\mathbf{w}}_0\|^2 \|\tilde{\mathbf{x}}\|^2}\right]}{E\left[\frac{e_{i,D}^2 \|\tilde{\mathbf{x}}\|^2}{\|\bar{\mathbf{w}}_0\|^4 \|\tilde{\mathbf{x}}\|^4} + \frac{2e_{i,D}^3 \tilde{\mathbf{x}}^T \mathbf{w}_0}{\|\bar{\mathbf{w}}_0\|^6 \|\tilde{\mathbf{x}}\|^4} + \frac{e_{i,D}^4 \mathbf{w}_0^T \mathbf{w}_0}{\|\bar{\mathbf{w}}_0\|^8 \|\tilde{\mathbf{x}}\|^4}\right]} \quad (A1)$$

From the paper [13] we have $\|\tilde{\mathbf{x}}\|^2 \approx (L-2)\sigma_{i,\tilde{\mathbf{x}}}^2$ and the length L of the subband adaptive filter is large, so (A1) can be further simplified as:

$$\frac{2E[\tilde{\mathbf{w}}(t)^T \hat{\mathbf{g}}_{TLMM-NSAF}(\mathbf{w}(t))]}{E[\hat{\mathbf{g}}_{TLMM-NSAF}(\mathbf{w}(t))^T \hat{\mathbf{g}}_{TLMM-NSAF}(\mathbf{w}(t))]} \approx 2 \frac{E\left[\frac{e_{i,D}^2}{\|\bar{\mathbf{w}}_0\|^2 \|\tilde{\mathbf{x}}\|^2}\right]}{E\left[\frac{e_{i,D}^2 \|\tilde{\mathbf{x}}\|^2}{\|\bar{\mathbf{w}}_0\|^4 \|\tilde{\mathbf{x}}\|^4}\right]} = 2(\|\mathbf{w}_0\|^2 + \theta_i) \quad (A2)$$

APPENDIX B

Using (40) we have:

$$\begin{aligned} & E[\mathbf{r}(\mathbf{w}_0)\mathbf{r}(\mathbf{w}_0)^T] \\ &= \sum_{i=0}^{N-1} E\left[\frac{e_{i,D}^2 \tilde{\mathbf{x}}_i(t) \tilde{\mathbf{x}}_i(t)^T}{\|\bar{\mathbf{w}}_0\|^4 \|\tilde{\mathbf{x}}_i(t)\|^4} + \frac{e_{i,D}^3(t) \mathbf{w}_0 \tilde{\mathbf{x}}_i(t)^T}{\|\bar{\mathbf{w}}_0\|^6 \|\tilde{\mathbf{x}}_i(t)\|^4} \right. \\ & \quad \left. + \frac{e_{i,D}^3(z) \tilde{\mathbf{x}}_i(z) \mathbf{w}_0^T}{\|\bar{\mathbf{w}}_0\|^6 \|\tilde{\mathbf{x}}_i(z)\|^4} + \frac{e_{i,D}^4(z) \mathbf{w}_0 \mathbf{w}_0^T}{\|\bar{\mathbf{w}}_0\|^8 \|\tilde{\mathbf{x}}_i(z)\|^4}\right] \end{aligned}$$

$$\begin{aligned} &= \frac{1}{\|\bar{\mathbf{w}}_0\|^4} \sum_{i=0}^{N-1} \left\{ \frac{E[e_{i,D}^2(t) \tilde{\mathbf{x}}_i(t) \tilde{\mathbf{x}}_i(t)^T]}{\|\tilde{\mathbf{x}}_i(t)\|^4} + \frac{E[e_{i,D}^3(t) \mathbf{w}_0 \tilde{\mathbf{x}}_i(t)^T]}{\|\bar{\mathbf{w}}_0\|^2 \|\tilde{\mathbf{x}}_i(t)\|^4} \right. \\ & \quad \left. + \frac{E[e_{i,D}^3(t) \tilde{\mathbf{x}}_i(t) \mathbf{w}_0^T]}{\|\bar{\mathbf{w}}_0\|^2 \|\tilde{\mathbf{x}}_i(t)\|^4} + \frac{E[e_{i,D}^4(t) \mathbf{w}_0 \mathbf{w}_0^T]}{\|\bar{\mathbf{w}}_0\|^4 \|\tilde{\mathbf{x}}_i(t)\|^4} \right\} \quad (B1) \end{aligned}$$

Using the properties of the kurtosis of the Gaussian distribution[5] and the assumptions 1, it is easy to verify that

$$\begin{aligned} E[e_{i,D}^2(t)] &= E[(v_i(t) - \mathbf{u}_i^T(t) \mathbf{w}_0)^2] \\ &= E[v_i(t)^2] + E[(\mathbf{u}_i^T(t) \mathbf{w}_0)^2] \quad (B2) \end{aligned}$$

$$= \sigma_i^2 \|\bar{\mathbf{w}}_0\|^2$$

and

$$\begin{aligned} E[e_{i,D}^4(t)] &= E[(v_i(t) - \mathbf{u}_i^T(t) \mathbf{w}_0)^4] \\ &= 3\left\{E[(v_i(t) - \mathbf{u}_i^T(t) \mathbf{w}_0)^2]\right\}^2 \\ &= 3\sigma_i^4 \|\bar{\mathbf{w}}_0\|^4 \quad (B3) \end{aligned}$$

Due to the mathematical definition of expectation, when a and b do not satisfy the independence condition, $E[ab] \neq E[a]E[b]$. Then the expected term in B1 is calculated as:

$$\begin{aligned} & E[e_{i,D}^2(t) \tilde{\mathbf{x}}_i(t) \tilde{\mathbf{x}}_i(t)^T] \\ &= E[(v_n - \mathbf{u}_i^T(t) \mathbf{w}_0)^2 \mathbf{R} + (v_n - \mathbf{u}_i^T(t) \mathbf{w}_0)^2 \tilde{\mathbf{x}}_i(t) \mathbf{u}_i^T(t) \\ & \quad + (v_n - \mathbf{u}_i^T(t) \mathbf{w}_0)^2 \mathbf{u}_i(t) \tilde{\mathbf{x}}_i(t)^T \\ & \quad + (v_n - \mathbf{u}_i^T(t) \mathbf{w}_0)^2 \mathbf{u}_i(t) \mathbf{u}_i^T(t))] \quad (B4) \\ &= \sigma_{i,in}^2 \|\bar{\mathbf{w}}_0\|^2 (\mathbf{R} + \sigma_{i,in}^2 \mathbf{I}) \end{aligned}$$

and

$$\begin{aligned} & E[(v_i(t) - \mathbf{u}_i^T(t) \mathbf{w}_0)^3 \tilde{\mathbf{x}}_i(t) \mathbf{w}_0^T] \\ &= E[v_i(t)^3 \mathbf{u}_i(t) \mathbf{w}_0^T - 3v_i(t)^2 (\mathbf{u}_i^T(t) \mathbf{w}_0) \mathbf{u}_i(t) \mathbf{w}_0^T \\ & \quad + 3v_i(t) (\mathbf{u}_i^T(t) \mathbf{w}_0)^2 \mathbf{u}_i(t) \mathbf{w}_0^T - (\mathbf{u}_i^T(t) \mathbf{w}_0)^3 \mathbf{u}_i(t) \mathbf{w}_0^T] \quad (B5) \\ &= -3\sigma_{i,in}^4 \|\bar{\mathbf{w}}_0\|^2 \mathbf{w}_0 \mathbf{w}_0^T \end{aligned}$$

in the same way, we have

$$E[(v_i(t) - \mathbf{u}_i^T(t) \mathbf{w}_0)^3 \mathbf{w}_0 \tilde{\mathbf{x}}_i(t)^T] = -3\sigma_{i,in}^4 \|\bar{\mathbf{w}}_0\|^2 \mathbf{w}_0 \mathbf{w}_0^T \quad (B6)$$

Where $\mathbf{R} = E[x_i(t) x_i^T(t)]$. Substituting (B3)–(B6) into (B1) results in (40).

REFERENCES

- [1] A. H. Sayed, *Fundamentals of Adaptive Filtering*. Hoboken, NJ, USA: Wiley, 2003.
- [2] A. Feuer and E. Weinstein, "Convergence analysis of LMS filters with uncorrelated Gaussian data," *IEEE Trans. Acoust., Speech, Signal Process.*, vol. 33, no. 1, pp. 222-230, Feb. 1985.

- [3] T. K. Paul and T. Ogunfunmi, "On the Convergence Behavior of the Affine Projection Algorithm for Adaptive Filters," *IEEE Trans. Circuits and Systems I: Regular Papers*, vol. 58, no. 8, pp. 1813-1826, Aug. 2011.
- [4] M. Z. A. Bhotto and A. Antoniou, "Affine-Projection-Like Adaptive-Filtering Algorithms Using Gradient-Based Step Size," *IEEE Trans. Circuits and Systems I: Regular Papers*, vol. 61, no. 7, pp. 2048-2056, Jul. 2014.
- [5] N. L. Johnson, S. Kotz, and N. Balakrishnan, *Continuous Univariate Distributions, 2nd ed.* New York, NY, USA: Wiley, 1994, vol. 1.
- [6] J. J. Jeong, S. H. Kim, G. Koo and S. W. Kim, "Mean-Square Deviation Analysis of Multiband-Structured Subband Adaptive Filter Algorithm," *IEEE Trans. Signal Processing*, vol. 64, no. 4, pp. 985-994, Feb. 15, 2016.
- [7] K. A. Lee and W. S. Gan, "Improving convergence of the NLMS algorithm using constrained subband updates," *IEEE Signal Processing Lett.*, vol. 11, no. 9, pp. 736-739, Sept. 2004.
- [8] M. De Courville and P. Duhamel, "Adaptive filtering in subbands using a weighted criterion," *IEEE Trans. Signal Processing*, vol. 46, no. 9, pp. 2359-2371, Sept. 1998.
- [9] H. Zhao, Y. Chen, J. Liu and Y. Zhu, "Total Least Squares Normalized Subband Adaptive Filter Algorithm for Noisy Input," *IEEE Trans. Circuits and Systems II: Express Briefs*, vol. 69, no. 3, pp. 1977-1981, Mar. 2022.
- [10] Y. Zhou, S. C. Chan and K. L. Ho, "New Sequential Partial-Update Least Mean M-Estimate Algorithms for Robust Adaptive System Identification in Impulsive Noise," *IEEE Trans. Ind. Electron.*, vol. 58, no. 9, pp. 4455-4470, Sept. 2011.
- [11] Chan, S.C., Zhou, Y. On the Performance Analysis of the Least Mean M-Estimate and Normalized Least Mean M-Estimate Algorithms with Gaussian Inputs and Additive Gaussian and Contaminated Gaussian Noises. *J Sign Process Syst Sign Image Video Technol* 60, 81 – 103 (2010).
- [12] Z. Zheng and H. Zhao, "Affine projection M-estimate subband adaptive filters for robust adaptive filtering in impulsive noise," *Signal Process.*, vol. 120, pp. 64 – 70, 2016.
- [13] Z. Zheng and Z. Liu, "Influence of input noises on the mean-square performance of the normalized subband adaptive filter algorithm," *J. Franklin Inst.*, vol. 357, no. 2, pp. 1318-1330, Feb. 2020.
- [14] Z. Zheng and H. Zhao, "Bias-Compensated Normalized Subband Adaptive Filter Algorithm," *IEEE Signal Processing Lett.*, vol. 23, no. 6, pp. 809-813, Jun. 2016.
- [15] Z. Zheng, Z. Liu, and X. Lu, "Robust normalized subband adaptive filter algorithm against impulsive noises and noisy inputs," *J. Franklin Inst.*, vol. 357, no. 5, pp. 3113–3134, Mar. 2020.
- [16] H. Zhao, D. Liu and S. Lv, "Robust Maximum Correntropy Criterion Subband Adaptive Filter Algorithm for Impulsive Noise and Noisy Input," *IEEE Trans. Circuits and Systems II: Express Briefs*, vol. 69, no. 2, pp. 604-608, Feb. 2022.
- [17] R. Arablouei, S. Werner and K. Doğançay, "Analysis of the Gradient-Descent Total Least-Squares Adaptive Filtering Algorithm," *IEEE Trans. Signal Processing*, vol. 62, no. 5, pp. 1256-1264, Mar. 2014.
- [18] L. Li and H. Zhao, "A Robust Total Least Mean M-Estimate Adaptive Algorithm for Impulsive Noise Suppression," *IEEE Trans. Circuits and Systems II: Express Briefs*, vol. 67, no. 4, pp. 800-804, Apr. 2020.
- [19] F. Wang, Y. He, S. Wang, and B. Chen, "Maximum total correntropy adaptive filtering against heavy-tailed noises," *Signal Processing.*, vol. 141, pp. 84–95, Dec. 2017.
- [20] H. Zhao, Y. Chen and S. Lv, "Robust Diffusion Total Least Mean M-estimate Adaptive Filtering Algorithm and Its Performance Analysis," *IEEE Trans. Circuits and Systems II: Express Briefs*, vol. 69, no. 2, pp. 654-658, Feb. 2022.
- [21] L. Lu, H. Zhao, and C. Chen, "A new normalized subband adaptive filter under minimum error entropy criterion," *SIGNAL IMAGE VIDEO P.*, vol. 10, no. 6, pp. 1097–1103, Sep. 2016.
- [22] C. T. Kelley, *Iterative Methods for Optimization*. Philadelphia, PA: SIAM, 1999, no. 18 in *Frontiers in Appl. Math.*
- [23] Y. Yu, H. He, B. Chen, J. Li, Y. Zhang and L. Lu, "M-Estimate Based Normalized Subband Adaptive Filter Algorithm: Performance Analysis and Improvements," *IEEE/ACM Trans. Audio, Speech, Lang. Process.*, vol. 28, pp. 225-239, 2020.
- [24] Yuxian Zou, Shing-Chow Chan and Tung-Sang Ng, "Least mean M-estimate algorithms for robust adaptive filtering in impulse noise," *IEEE Trans. Circuits and Systems II: Analog and Digital Signal Processing*, vol. 47, no. 12, pp. 1564-1569, Dec. 2000.
- [25] Y. Yu and H. Zhao, "Incremental M-estimate-based least-mean algorithm over distributed network," *Electron. Lett.*, vol. 52, no. 14, pp. 1270 – 1272, Jul. 2016.
- [26] Y. Zhou, S. C. Chan and K. L. Ho, "New Sequential Partial-Update Least Mean M-Estimate Algorithms for Robust Adaptive System Identification in Impulsive Noise," *IEEE Trans. Ind. Electron.*, vol. 58, no. 9, pp. 4455-4470, Sept. 2011.
- [27] J. J. Jeong, S. H. Kim, G. Koo and S. W. Kim, "Mean-Square Deviation Analysis of Multiband-Structured Subband Adaptive Filter Algorithm," *IEEE Trans. Signal Processing*, vol. 64, no. 4, pp. 985-994, Feb. 15, 2016.
- [28] K. M. Abadir, J. R. Magnus. *Matrix algebra [M]*. Cambridge University Press, 2005.
- [29] R. H. Kwong and E. W. Johnston, "A variable step size LMS algorithm," *IEEE Trans. Signal Processing*, vol. 40, no. 7, pp. 1633-1642, Jul. 1992.
- [30] J. Arenas-Garcia, A. R. Figueiras-Vidal and A. H. Sayed, "Mean-square performance of a convex combination of two adaptive filters," *IEEE Trans. Signal Processing*, vol. 54, no. 3, pp. 1078-1090, Mar. 2006.
- [31] J. Ni and F. Li, "Adaptive combination of subband adaptive filters for acoustic echo cancellation," *IEEE T CONSUM ELECTRON.*, vol. 56, no. 3, pp. 1549-1555, Aug. 2010.
- [32] Y. Yu and H. Zhao, "Incremental M-estimate-based least-mean algorithm over distributed network," *Electron. Lett.*, vol. 52, no. 14, pp. 1270 – 1272, Jul. 2016.
- [33] V. Mathews and S. Cho, "Improved convergence analysis of stochastic gradient adaptive filters using the sign algorithm," *IEEE Trans. Acoust., Speech, Signal Process.*, vol. ASSP-35, no. 4, pp. 450 – 454, Apr. 1987.
- [34] J.-H. Kim, J. Kim, J. H. Jeon, and S. W. Nam, "Delayless individual-weighting-factors sign subband adaptive filter with band-dependent variable step-sizes," *IEEE/ACM Trans. Audio, Speech, Lang. Process.*, vol. 25, no. 7, pp. 1526 – 1534, Jul. 2017.
- [35] J. Ni and F. Li, "A variable step-size matrix normalized subband adaptive filter," *IEEE Trans. Audio, Speech, Lang. Process.*, vol. 18, no. 6, pp. 1290 – 1299, Aug. 2010.